Thermochimica Acta, 142 (1989) 29–47
Elsevier Science Publishers B.V., Amsterdam – Printed in The Netherlands

STRUCTURAL RELAXATION, GLASS TRANSITION AND CRYSTALLIZATION OF Cu–Zr AMORPHOUS RIBBONS STUDIED BY DILATOMETRY AND DIFFERENTIAL SCANNING CALORIMETRY

E. ETCHESSAHAR

Laboratoire de Métallurgie et Physico-Chimie des Matériaux, Institut National des Sciences Appliquées, 20, Avenue des Buttes de Coësmes, 35031 Rennes Cedex (France)

M. HARMELIN

CNRS, Centre d'Etudes de Chimie Métallurgique, 15, rue Georges Urbain, 94407 Vitry-sur-Seine Cedex (France)

J. DEBUIGNE

Laboratoire de Métallurgie et Physico-Chimie des Matériaux, Institut National des Sciences Appliquées, 20, Avenue des Buttes de Coësmes, 35031 Rennes Cedex (France)

(Received 31 May 1988)

ABSTRACT

The structural relaxation, glass transition and crystallization of $Cu_{33}Zr_{67}$, $Cu_{40}Zr_{60}$ and $Cu_{60}Zr_{40}$ amorphous ribbons were studied by dilatometry and differential scanning calorimetry (DSC). A highly sensitive dilatometer (built by us) was used which allowed samples in the form of thin ribbon to be heated at a slow heating rate ($1.7\,^{\circ}C\ min^{-1}$) in an ultrahigh vacuum (10^{-9} Torr). Thermal expansion coefficients were determined on heating and cooling. Isothermal annealings were also performed in situ in the dilatometer. The mean coefficients of linear thermal expansion ($\alpha \times 10^6$) measured for the relaxed amorphous alloys and for the crystalline alloys were the same between room temperature and the crystallization temperature: 9.2 ± 0.2 for $Cu_{33}Zr_{67}$, 9.9 ± 0.2 for $Cu_{40}Zr_{60}$ and 11.8 ± 0.2 for $Cu_{60}Zr_{40}$. The increase in the coefficient of thermal expansion is thus strongly correlated with the increase in copper content. These values are very close to those calculated assuming a linear relationship between the mean composition and the values of α_m of the individual components. This suggests that the cohesion varies smoothly with composition without any substantial change in the nature of bonding.

After the initial heating of the as-quenched ribbons below the glass transition, structural relaxation resulted in shrinkage of the samples after cooling to room temperature. The glass transition was indicated by the creep of the specimen. Crystallization resulted in an important shrinkage.

DSC was used to aid in the interpretation of the dilatometric events, in particular for the characterization of the enthalpy relaxation associated with structural relaxation and of the enthalpy increase at the glass transition. The irreversibility of the structural relaxation below the glass transition was clearly demonstrated by DSC as were the reversible enthalpy changes at the glass transition.

0040-6031/89/$03.50

INTRODUCTION

Structural relaxation phenomena associated with heat treatments below or near the glass transition temperature have been reported for liquid-quenched Cu–Zr amorphous alloys in previous papers [1–4]. Two major effects have been observed using differential scanning calorimetry (DSC): (i) an exothermic (irreversible) phenomenon during the initial heating of the as-quenched specimen; (ii) an endothermic phenomenon in the glass transition region of the pre-annealed specimens. The intensity of the endothermic phenomenon has been shown to be dependent on the decrease in the configurational enthalpy ΔH_a during the annealing treatment. The exothermic phenomenon is consistent with a large spectrum of relaxation times [3,5]. Recent dilatometric experiments carried out on amorphous $Fe_{78}B_{13}Si_9$ alloys [6] have shown that this phenomenon is accompanied by the shrinkage of the amorphous ribbons and is mainly associated with the annealing out of the excess free volume of the as-quenched samples.

The aim of this work is to report the results obtained during precise thermal expansion measurements on Cu_xZr_{100-x} ($x = 33$, 40, 60). The Cu–Zr system is rather remarkable for a number of reasons: (i) it is among the rare metal–metal alloys which allow glass formation by liquid quenching over a wide composition range [7]; (ii) the glass transition is clearly shown on the DSC curves for all compositions; (iii) amorphous samples can be heated in the glass temperature region without crystallization [4]. However, it is particularly important to note that oxygen contamination occurs readily in the amorphous ribbons of this system, even under nominally pure argon [8]. As the results reported in this paper were obtained using a dilatometer which allows samples in the form of thin ribbon to be heated in an ultrahigh vacuum (10^{-9} Torr) [9], oxygen contamination of the Cu–Zr ribbons was completely avoided. Consequently, the results obtained and discussed below are related to the structural relaxation processes characteristic of the Cu–Zr system and not to artefacts resulting from oxygen contamination. As the only data reported in the literature for the Cu–Zr system are those obtained by Fritsch et al. [10] for $Cu_{40}Zr_{60}$ from 240 to 280 K, such direct dilatometric measurements on continuous heating from room temperature to 600 °C in an ultrahigh vacuum are the first to be performed on Cu–Zr-based amorphous ribbons.

Differential scanning calorimetric measurements were used to aid in the interpretation of the dilatometric events and in their correlation with (i) structural relaxation, (ii) the glass transition and (iii) crystallization. The DSC technique has been revealed as a very powerful tool for such purposes in various papers [1–4,11,12].

EXPERIMENTAL

The starting ingots with compositions $Cu_{33}Zr_{67}$, $Cu_{40}Zr_{60}$ and $Cu_{60}Zr_{40}$ were prepared by levitation melting in a purified helium atmosphere. The ingots were then broken up and fragments (≈ 3 g) were quenched from the liquid state by the planar-flow-casting technique on a copper wheel in a pre-evacuated tank, again in purified helium. Ribbons were typically ≈ 7 mm wide and 30 μm thick. These ribbons were checked by X-ray diffraction using Co $K\alpha$ radiation and a diffracted beam graphite monochromator. No traces of Bragg peaks were detected: the results presented here were obtained from fully amorphous specimens.

Dilatometric measurements

For carrying out thermal expansion measurements on thin and flexible metallic ribbons, the sample holder must be of the tensile type and must comply with the following criteria: (i) the sample must be fixed in a unique plane of the space, (ii) the dimensional changes must be transmitted without slipping at the clamps, (iii) expansion phenomena must not be reduced and (iv) no reaction must occur between the sample holder and the sample.

Our sample holder, which is made of transparent silica, satisfies these requirements. A description is given in Fig. 1. The sample (1) was previously punched along the longitudinal axis with two holes of 3 mm in diameter. The sample holder consists of three main parts.

(a) A bulky part (2) joined to the end of a fixed silica tube. Part (2) is composed of a fixed clip (3) and four strictly parallel guiding surfaces ((4), (5), (6), (7)).

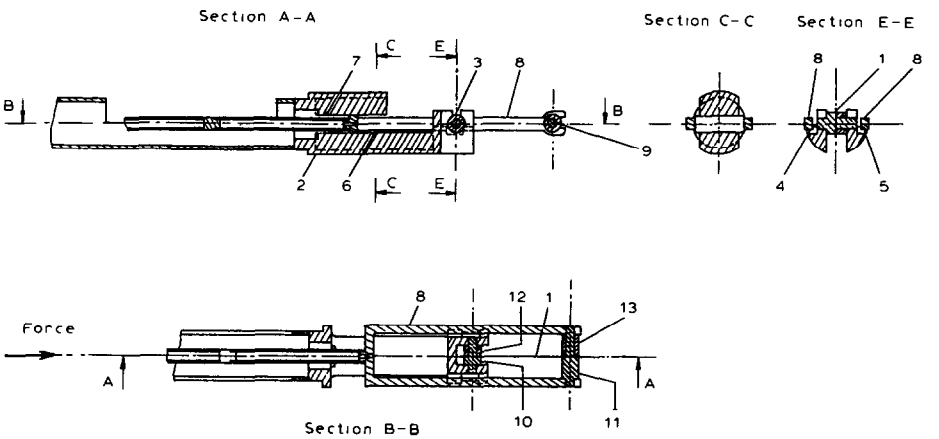

Fig. 1. Description of the sample holder used for the thermal expansion measurements.

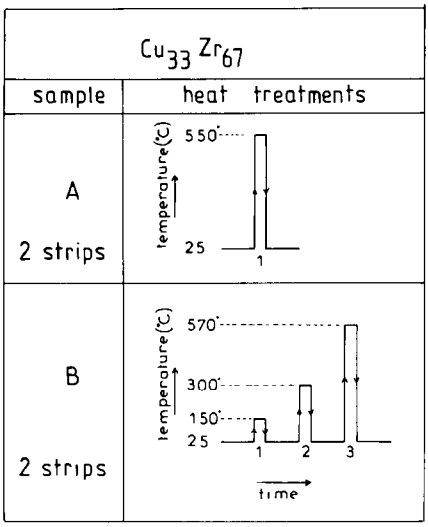

Fig. 2. Description of the thermal heat treatments successively applied to the $Cu_{33}Zr_{67}$ amorphous alloys (samples A and B). Dilatometric samples: heating rate and cooling rate, 1.7 °C min^{-1}; DSC samples: heating rate, 40 °C min^{-1}; cooling rate, 320 °C min^{-1}. Time of isothermal treatments at 150, 300, 550 and 570 °C: 5 min.

(b) A "U-form" sliding clip (8), perfectly parallel, composed of a clip (9) which slides along the pressure axis in the planes (4), (5), (6) and (7) of the fixed part. The elastic pressure is delivered by a tubular push-rod.

(c) Two cylindrical axes (10) and (11) of different lengths, with stoppers and cross-pieces, mounted firmly on the sample. The smallest (10) is bound to the fixed clip and the largest (11) is bound to the sliding clip. The cross-pieces (12) and (13) are used as radial clip-stoppers.

Samples of length 40 mm were used and a tensile stress of 5×10^4 Pa was applied to them during the experiment.

This sample holder was adapted to the dilatometer described elsewhere [9]. This dilatometer is a direct type. Samples were heated in an ultrahigh vacuum (10^{-9} Torr). The specific heat treatments applied to the different samples in the dilatometer and the number of strips used for each experiment are shown in Fig. 2 for $Cu_{33}Zr_{67}$, in Fig. 3 for $Cu_{40}Zr_{60}$ and in Fig. 4 for $Cu_{60}Zr_{40}$. Two strips were generally used with the exception of $Cu_{40}Zr_{60}$ (sample D, one strip) and $Cu_{60}Zr_{40}$ (sample F, one strip).

DSC measurements

A Perkin–Elmer differential scanning calorimeter (DSC-2C) connected to a 3600 thermal analysis data station was used. Each specimen ($\approx$ 20 mg) was enclosed in a copper pan. Crystallized samples were used as reference. The atmosphere was pure argon. The heating rate was 40 °C min^{-1}. In order to

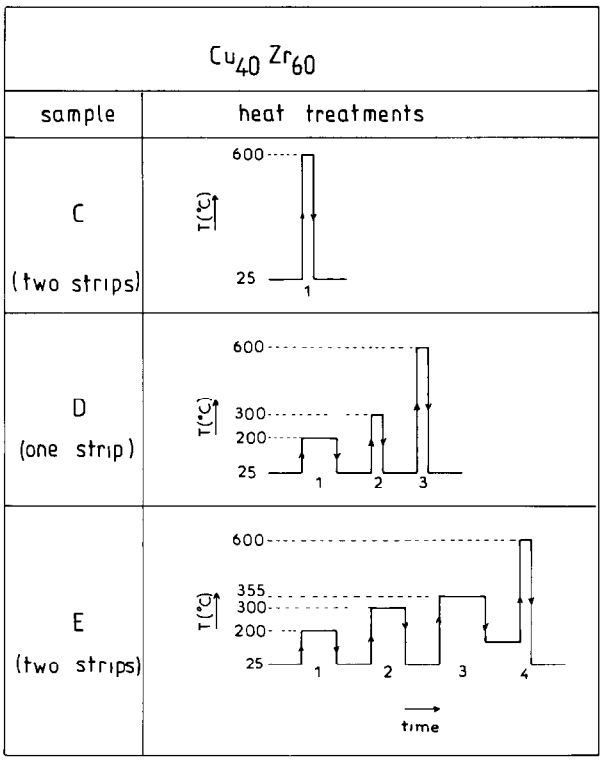

Fig. 3. Description of the thermal heat treatments successively applied to the $Cu_{40}Zr_{60}$ amorphous alloys (samples C, D and E). Dilatometric samples: heating rate and cooling rate, 1.7 °C min^{-1}; DSC samples: heating rate, 40 °C min^{-1}; cooling rate, 320 °C min^{-1}. Time of isothermal treatments: at 200 °C, 30 min; at 300 °C, 5 min (D2) or 30 min (E2); at 355 °C, 45 min; at 600 °C, 5 min.

eliminate the drift of the baseline the following procedure was used. For a given specimen, after the series of successive heat treatments shown in the figures had been performed, two supplementary runs from room temperature to the upper temperature (generally 600 °C) were successively carried out with the crystallized specimen to check the reproducibility of the baseline. These last two runs were then subtracted from each other and a straight line was obtained, denoted A_x, B_x, $C_x \ldots$, E_x in the figures. In the same way, the first curve obtained with the as-quenched sample (denoted by index 1, e.g. A_1) was derived after subtraction from the last curve obtained with the same specimen in the crystallized state. The curves A_x, $B_x, \ldots$, E_x were used as reference to delimit the heat effects due to structural relaxation, glass transition and crystallization. This procedure enabled us to check the reliability of each series of DSC experiments and to eliminate completely the thermal drift of the baseline due to the specific conditions of heat transfer between the sample and the temperature sensor of the DSC cell. All the

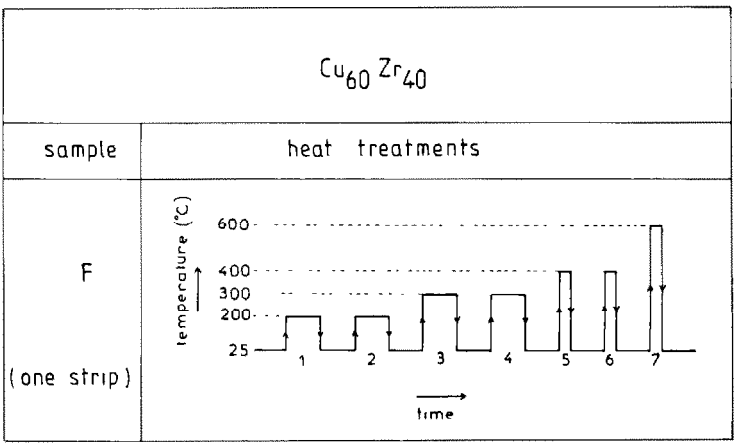

Fig. 4. Description of the thermal heat treatments successively applied to the $Cu_{60}Zr_{40}$ amorphous alloys (sample F). Dilatometric sample: heating rate and cooling rate, 1.7 °C min^{-1}. Time of isothermal treatments: at 200 °C, 30 min; at 300 °C, 30 min (F3) and 45 min (F4); at 400 and 600 °C, <1 min.

DSC curves shown in the figures are normalized to 1 mg sample weight and are plain copies of the originals.

RESULTS AND DISCUSSION

$Cu_{33}Zr_{67}$

The dilatometric curve obtained with sample A on heating up to 550 °C and cooling to room temperature is shown in Fig. 5. From room temperature to 130 °C, the thermal expansion is linear with a mean coefficient $\alpha_{m,h} = 9.1 \times 10^{-6}$ (Table 1). From 130 to 280 °C, the thermal expansion is lower and is no longer linear; it has an apparent value of $\alpha_{m,a} = 7.5 \times 10^{-6}$. From 280 to 360 °C, an important increase in sample length is observed ($\Delta L/L = +22 \times 10^{-4}$) (Table 2). From 360 to 380 °C, the sample length decreases ($\Delta L/L = -1.2 \times 10^{-5}$). On cooling from 550 °C, the decrease in sample length is linear down to room temperature ($\alpha_{m,c} = 9.1 \times 10^{-6}$) (Table 3).

This dilatometric behaviour may be understood and interpreted by comparison with the DSC curve of Fig. 6 which shows: (i) an exothermic phenomenon from $\approx$ 110 to 300 °C; (ii) an endothermic deviation from $\approx$ 300 to 370 °C; (iii) a sharp exothermic effect between $\approx$ 370 and 410 °C followed by a broad exothermic effect up to 600 °C.

From these results, it can be concluded that: (i) the decrease in the mean thermal expansion coefficient between $\approx$ 130 and 280 °C (Fig. 5) is due to structural relaxation, (ii) the increase in length between 300 and 370 °C is due to creep caused by the decrease in sample viscosity in the glass

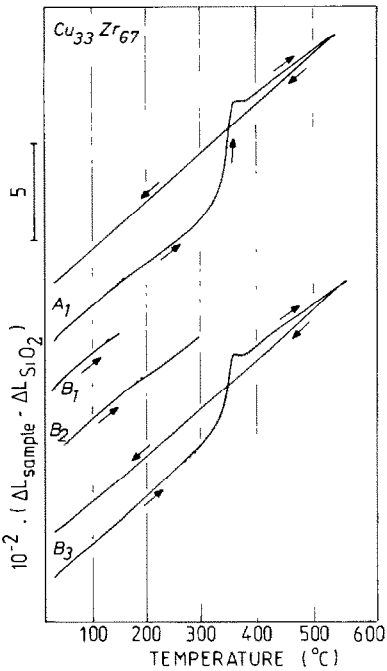

Fig. 5. Dilatometric curves of $Cu_{33}Zr_{67}$ amorphous alloys on heating and cooling samples A and B as described in Fig. 2.

transition temperature region and (iii) the decrease in sample length above 370 °C is due to crystallization [7,13,14].

The series of experiments carried out with sample B (Fig. 2 and Fig. 5) were performed in order to identify more precisely the nature of the phenomenon of structural relaxation below 280 °C. The irreversibility of the dilatometric thermal behaviour between 130 and 280 °C is proved by the experiments B_1, B_2 and B_3 as shown in Fig. 5. On heating sample B to 150

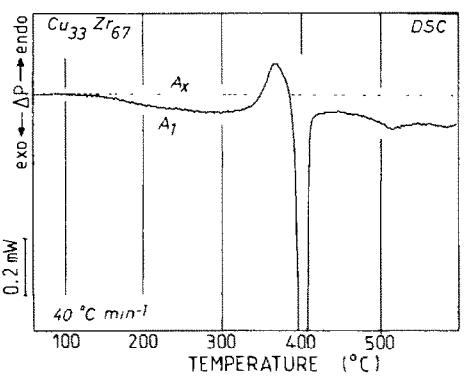

Fig. 6. DSC curve of the $Cu_{33}Zr_{67}$ amorphous alloy.

TABLE 1

Mean coefficients of linear thermal expansion ($\alpha_m \times 10^6$) of Cu–Zr amorphous ribbons on heating and cooling as described in Figs. 1, 2 and 3

Alloy	Sample		Heat cycle	Heating				Cooling		$\Delta L/L$ at 25 °C (10^{-4})
	Ref.	n		No relaxation		Relaxation range		T_4-T_5	$\alpha_{m,c}$	
				T_1-T_2 (°C)	$\alpha_{m,h}$	T_2-T_3 (°C)	$\alpha_{m,a}$			
$Cu_{33}Zr_{67}$	A	2	1	60–130	9.1	130–280	7.5	(530–60) [a]	9.1	n.m.
	B	2	1	60–120	8.6	120–150	7.0	150–60	9.2	n.m.
			2	60–175	8.9	175–300	6.9	300–60	9.1	−3.6
			3	60–300	9.0	–		(550–60) [a]	9.2	n.m.
$Cu_{40}Zr_{60}$	C	2	1	60–150	9.2	150–320	8.1	(600–60) [a]	9.6	n.m.
	D	1	1	60–185	9.2	185–200	8.3	200–60	9.9	−0.4
			2	60–240	9.4	240–300	7.9	300–60	10.0	−1.6
			3	60–200	9.2	–		(600–60) [a]	9.8	n.m.
	E	2	1	60–200	8.6	n.m.		200–60	9.7	−0.9
			2	60–230	9.0	230–300	7.4	300–150	9.9	−2.3
			3	60–300	9.3	–		300–60	10.0	n.m.
			4	n.m.		n.m.		(600–60) [a]	9.9	n.m.
$Cu_{60}Zr_{40}$	F	1	1	25–160	n.m.	160–200	n.m.	200–50	11.0	n.m.
			2	50–200	10.5	–	–	200–50	11.1	0
			3	50–240	10.8	240–300	9.3	300–50	11.4	−2.6
			4	50–300	10.9	–	–	300–50	11.4	0
			5	50–340	11.2	340–400	10.7	400–50	11.6	−0.9
			6	50–400	11.5	–	–	400–50	11.8	0
			7	50–400	11.7	–	–	(600–50) [a]	12.6	n.m.

[a] Crystallized state. $\alpha_{m,h}$, mean coefficient on heating; $\alpha_{m,c}$, mean coefficient on cooling; $\alpha_{m,a}$, apparent mean coefficient during structural relaxation; n.m., not measured; n, number of strips.

TABLE 2

Dilatometric behaviour of Cu–Zr amorphous ribbons during glass transition

Alloy	Sample		Heat cycle	Glass transition temperature range $T_{g_1} - T_{gf}$ (°C)	Creep $[\Delta L/L]_i^f$ (10^{-4})
	Ref.	n			
$Cu_{33}Zr_{67}$	A	2	1	≈ 280–360	+22.3
	B	2	3	≈ 280–360	+14.5
$Cu_{40}Zr_{60}$	C	2	1	≈ 360–390	+8.2
	D	1	3	≈ 330–390	+53.0
	E	2	3	$T = 355$ °C	+7.2
	E	2	4	≈ 350–380	+19.2
$Cu_{60}Zr_{40}$	F	1	7	≈ 420–450	+18.3

and 300 °C successively, it is observed (after cooling to room temperature from these respective temperatures and heating again) that this phenomenon is irreversible, corresponds to a residual shrinkage after cooling to room temperature (e.g. $\Delta L/L = -3.6 \times 10^{-4}$ after cycle B_2) and starts again above the previous upper limit temperature, e.g. at 175 °C for B_2.

The irreversibility of the exothermic effect revealed on the DSC curves between ≈ 110 and 300 °C is also indicated in Fig. 7. The same heat treatments as those described in Fig. 2 for the dilatometric sample B were applied to the DSC sample which is also denoted B. After the DSC sample B_1 was cooled from 150 °C, no exothermic effect was detected below 150 °C with B_2. The exothermic effect only developed above 150 °C. When sample B_2 was cooled from 300 °C and heated again to crystallization (B_3), no

TABLE 3

Dilatometric behaviour of Cu–Zr amorphous ribbons during and after crystallization

Alloy	Sample		Heat cycle	Crystallization range		After crystallization			
	Ref.	n		$T_{x_1} - T_{xf}$ (°C)	$\Delta L/L$ (10^{-5})	Heating		Cooling	
						$T_6 - T_7$ (°C)	$\alpha_{m,h}$ (10^{-6})	$T_8 - T_9$ (°C)	$\alpha_{m,c}$ (10^{-6})
$Cu_{33}Zr_{67}$	A	2	1	360–380	−1.2	430–550	7.5	500–60	9.1
	B	2	3	360–380	−2.4	380–550	7.4	550–60	9.2
$Cu_{40}Zr_{60}$	C	2	1	390–400	−110	–	–	600–60	9.6
	D	1	3	390–400	n.m.	–	–	600–60	9.8
	E	2	3	380–400	−143	–	–	600–60	9.9
$Cu_{60}Zr_{40}$	F	1	7	450–490	−61	550–600	12.6	600–60	12.6

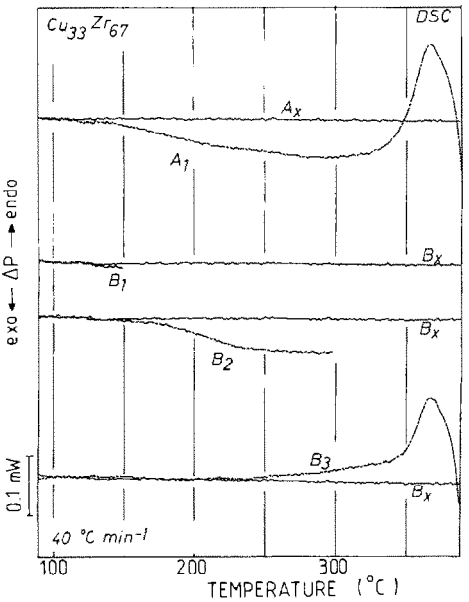

Fig. 7. DSC curves of $Cu_{33}Zr_{67}$ amorphous alloys on heating and cooling samples A and B as described in Fig. 2. The A_x and B_x traces correspond to the crystallized samples.

exothermic effect was observed below 300 °C with B_3 and the glass transition was revealed between ≈ 240 and 370 °C.

Another series of DSC experiments, described in Fig. 8, also demonstrate the irreversibility of the exothermic effect observed with the amorphous sample in the as-quenched state and the reversibility of the glass transition.

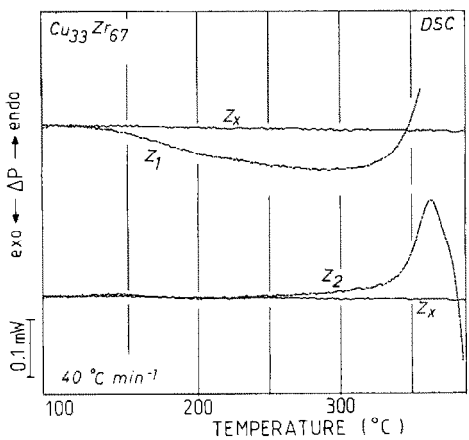

Fig. 8. DSC curves of $Cu_{33}Zr_{67}$ amorphous alloy (sample Z). The first heating (Z_1) was stopped in the glass transition range (370 °C) and the sample was immediately cooled to room temperature at 320 °C min^{-1}. Z_2 was the second run of the same sample. Z_x corresponds to the crystallized specimen.

Sample Z was first heated (Z_1) in the glass transition region (370 °C) and was then rapidly cooled (320 °C min^{-1}) to room temperature. The sample was then heated again (Z_2) to crystallization. The exothermic effect below 300 °C disappeared. The glass transition was clearly revealed between 240 and 370 °C as in Fig. 7.

Thus, the large increase in sample length observed between 280 and 380 °C on the dilatometric curves of samples A and B corresponds to the glass transition of the sample. Because the glass transition is accompanied by a strong decrease in the sample viscosity and because a small tensile stress is applied to the dilatometric sample, the glass transition is revealed on the dilatometric curves as a creep of the sample.

The mean coefficients of linear thermal expansion measured for the series of experiments carried out with $Cu_{33}Zr_{67}$ are reported in Table 1. It can be seen that the values of $\alpha_{m,c}$ remain constant ($(9.1 \pm 0.1) \times 10^{-6}$) and are the same as those of the crystallized sample.

The changes in length due to the glass transition and crystallization are listed in Tables 2 and 3, respectively.

$Cu_{40}Zr_{60}$

The dilatometric curve obtained with sample C on heating up to 600 °C and then cooling to room temperature is shown in Fig. 9. The thermal expansion is linear from 25 to 150 °C, with a mean coefficient $\alpha_{m,h} = 9.2 \times$

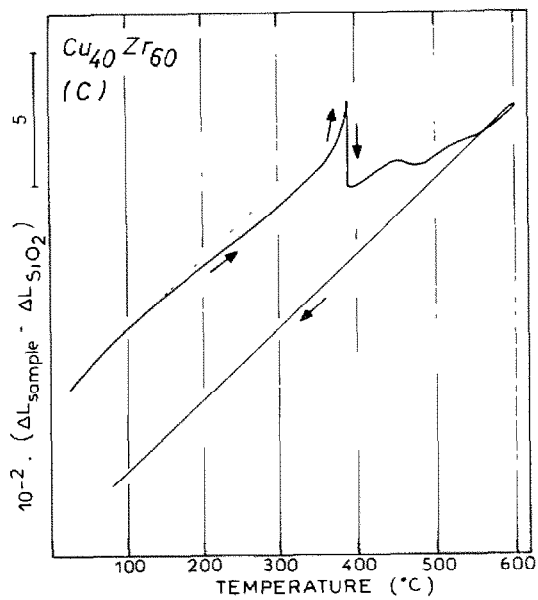

Fig. 9. Dilatometric curve of $Cu_{40}Zr_{60}$ amorphous alloys (sample C, as described in Fig. 3).

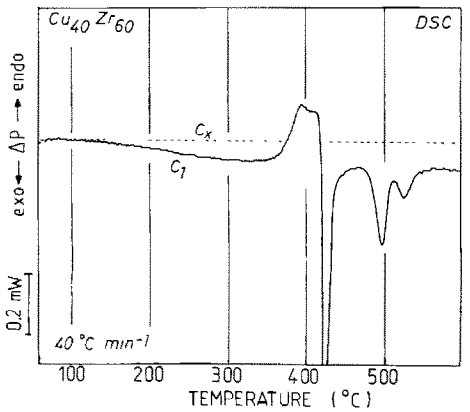

Fig. 10. DSC curve of $Cu_{40}Zr_{60}$ amorphous alloys.

10^{-6} (Table 1). Between 150 °C and 320 °C, the thermal expansion is no longer linear and the apparent value $\alpha_{m,a}$ (8.1×10^{-6}) is smaller than that below 150 °C. Then, from 320 to 390 °C, an important increase in sample length is observed ($\Delta L/L = +8 \times 10^{-4}$). From 390 to 400 °C, the sample length decreases rapidly ($\Delta L/L = -110 \times 10^{-5}$). From 390 to 550 °C, various discontinuities are observed until stabilization above 550 °C. On cooling from 600 °C to room temperature, the decrease in sample length is linear ($\alpha_{m,c} = 9.6 \times 10^{-6}$).

The dilatometric behaviour of sample C may be understood by comparison with the DSC curve illustrated in Fig. 10 which shows: (i) an exothermic phenomenon from 120 to 350 °C, due to the relaxation enthalpy of the as-quenched specimen on heating; (ii) an endothermic deviation from 350 to 400 °C corresponding to the glass transition; (iii) a sharp exothermic effect between 410 and 430 °C corresponding to crystallization. The broken line indicates that no further transformation occurs on reheating the same (crystallized) specimen after cooling from 600 °C to room temperature.

Thus the overall DSC behaviour of $Cu_{40}Zr_{60}$ is similar to that of $Cu_{33}Zr_{67}$. The changes in the temperatures of the corresponding phenomena and the differences in the crystallization processes are due to the differences in chemical composition [7,13,14]. As for $Cu_{33}Zr_{67}$, the DSC results allow us to conclude that the decrease in the mean thermal expansion coefficient between 150 and 320 °C (Fig. 9 and Table 1) is due to structural relaxation.

The series of experiments carried out with samples D and E were performed in order to check the influence of the number of strips used for the dilatometric sample on the corresponding results. Indeed, because a small tensile stress is applied to the sample during the dilatometric experiment, a possible effect of the number of strips on the amplitude of the creep at the glass transition can be expected . Evidence of such an effect is clearly given in Fig. 11 (sample D, cycle 3) which corresponds to a sample with only

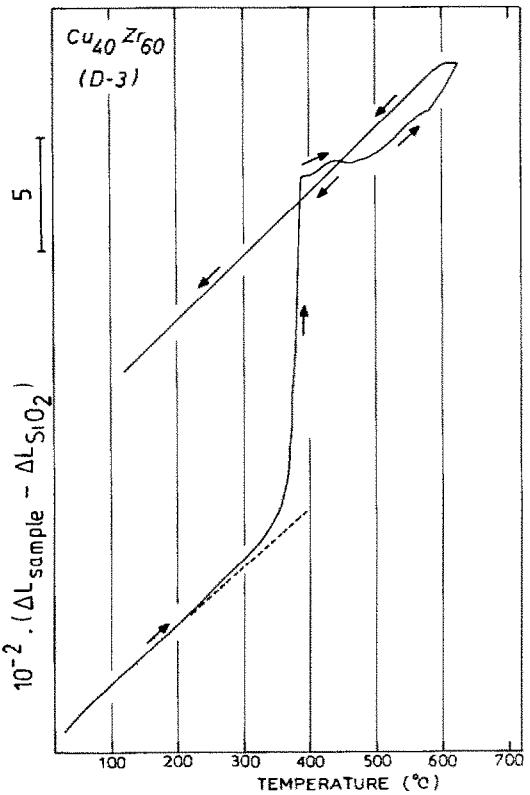

Fig. 11. Dilatometric curve of $Cu_{40}Zr_{60}$ amorphous alloys (sample D, as described in Fig. 3). Sample D3 is in a relaxed state after the previous D1 and D2 heat treatments. As only one strip was used for the dilatometric experiments, creep at the glass transition is particularly high.

one strip. The creep magnitude at T_g is much larger ($\Delta L/L = +53 \times 10^{-4}$) than when two strips are used (sample C, $\Delta L/L = +8 \times 10^{-4}$). However, it is important to note that the mean coefficients of linear thermal expansion remain unaffected by the number of strips both for the amorphous specimens (Table 1) and the crystallized specimens (Table 3).

The series of experiments carried out with samples D and E for $Cu_{40}Zr_{60}$ confirm the conclusions obtained with samples A and B for $Cu_{33}Zr_{67}$, i.e. (i) the dilatometric behaviour is irreversible below the glass transition, (ii) a residual shrinkage of the amorphous samples occurs at room temperature after cooling from 200 and 300 °C and (iii) identical values of $\alpha_{m,c}$ are obtained in the relaxed and crystallized states ($9.9 \pm 0.1) \times 10^{-6}$ for $Cu_{40}Zr_{60}$).

Cycle 3 with sample E (Fig. 12) was a special dilatometric experiment performed at constant temperature in the glass transition region in order to follow the isothermal creep of the sample. After such an annealing treatment at T_g (for 45 min at 355 °C) the glass transition was still observed on

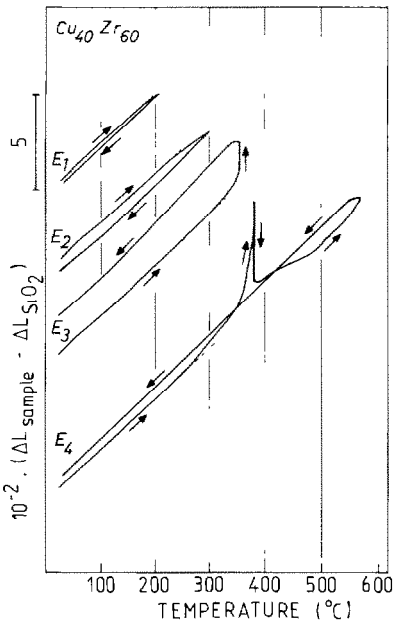

Fig. 12. Dilatometric curves of $Cu_{40}Zr_{60}$ amorphous alloys on heating and cooling sample E as described in Fig. 3.

reheating (cycle E_4), but crystallization occurred rapidly. Such a sharpness in crystallization can probably be explained by the combined effects of crystal nuclei formed during cycle 3 and of a supplementary driving force due to the tensile stress applied to the sample which facilitates the rapid growth of the nuclei.

Figure 13 shows the DSC curves obtained with $Cu_{40}Zr_{60}$ when the same heat treatments as those described in Fig. 3 were applied to the DSC samples C and E. Evidence of an exothermic effect is clearly seen for sample C from 120 °C to the glass transition. The irreversibility of this effect after 30 min at 200 °C is shown in curve E_2. Curve E_2 also shows a small endothermic phenomenon above 200 °C in agreement with Inoue et al. [2]. After 30 min at 300 °C, the exothermic effect is completely eliminated (E_3) and the glass transition starts smoothly from 250 °C. The slight difference between the starting temperatures of the DSC and dilatometric curves is due to the lower sensitivity of the dilatometric test compared with DSC. The increase in the endothermic peak at T_g after annealing for 45 min at 355 °C in the DSC cell is clearly seen in the DSC curve E_4. This increase is interpreted as being due to the enthalpy decrease of the amorphous sample during the isothermal annealing [4,11,12].

The irreversibility of the exothermic effect observed on initial heating of the as-quenched $Cu_{40}Zr_{60}$ amorphous sample and the reversibility of the glass transition can be seen in Fig. 14. Sample Y was initially heated (Y_1) in

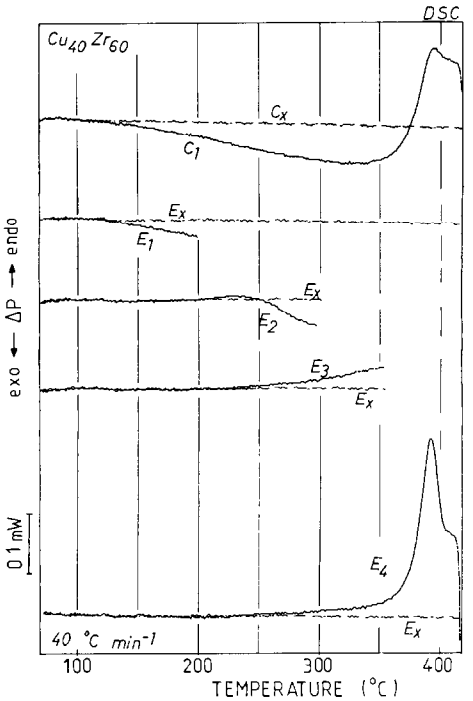

Fig. 13. DSC curves of $Cu_{40}Zr_{60}$ amorphous alloys on heating and cooling samples C and E as described in Fig. 3. The C_x and E_x traces correspond to the crystallized samples.

the glass transition region (380 °C) and rapidly cooled to room temperature. It was then heated again (Y_2) to crystallization. The exothermic effect disappeared and the glass transition was clearly revealed between 250 and 400 °C.

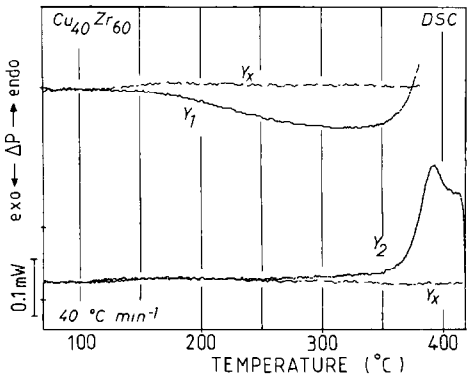

Fig. 14. DSC curves of the $Cu_{40}Zr_{60}$ amorphous alloy (sample Y). The first heating (Y_1) was stopped in the glass transition range (380 °C) and the sample was immediately cooled to room temperature at 320 °C min^{-1}. Y_2 was the second run of the same sample. Y_x corresponds to the crystallized specimen.

$Cu_{60}Zr_{40}$

The specific heat treatments applied to sample F in the dilatometer are described in Fig. 4. The aims of the successive thermal cycles to 200 °C (cycles 1 and 2), 300 °C (cycles 3 and 4), 400 °C (cycles 5 and 6) and 600 °C (cycle 7) were as follows: (i) to provide precise evidence of the effects of structural relaxation, glass transition and crystallization on the dilatometric behaviour of the sample and (ii) to determine whether the phenomena measured on heating were reproducible (and thus, reversible on cooling) or not.

The corresponding results are summarized in Tables 1, 2 and 3. The dilatometric curve corresponding to cycle 7 is shown in Fig. 15.

During the initial heating (cycle 1) of the as-quenched sample, structural relaxation starts at 160 °C and is irreversible on cooling. During cycle 2, the mean coefficients of linear thermal expansion measured on heating and cooling are approximately the same and no shrinkage is observed after the complete run (which includes an annealing treatment for 30 min at 200 °C) after cooling to room temperature. This means that the sample length is totally stabilized after cycle 1 in this range of temperature. During cycle 3, structural relaxation starts again at 240 °C. No further sample shrinkage is observed during the isothermal annealing for 30 min at 300 °C. This result is in agreement with those previously obtained with iron-based amorphous

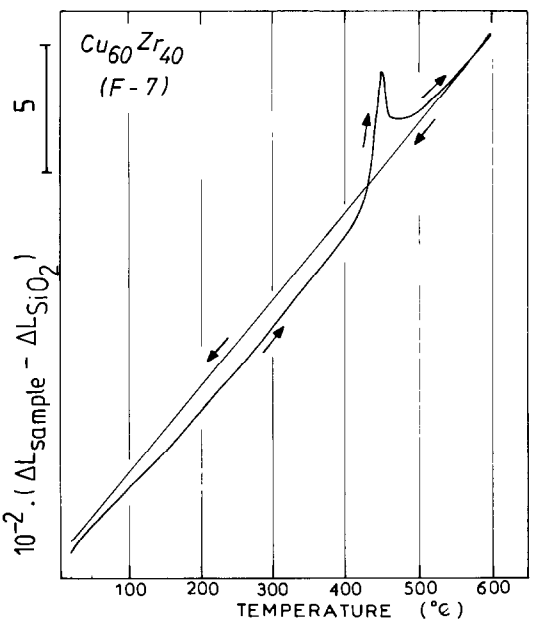

Fig. 15. Dilatometric curve of the $Cu_{60}Zr_{40}$ amorphous alloy (sample F, as described in Fig. 4). The sample F7 is in a relaxed state after the previous F1–F6 heat treatments.

ribbons (ref. 6, Fig. 3 and Table 1), i.e. below the glass transition, the sample length is in almost complete equilibrium on heating in the whole temperature range of structural relaxation.

Influence of the chemical composition on the mean coefficients of linear thermal expansion

The values of α_m are summarized in Table 4 for the three compositions investigated in this work, in the amorphous (relaxed) and crystalline states. Table 4 also compares these experimental values with the corresponding mean values calculated assuming a linear relationship between the mean composition and the values of α_m of the individual components (16.6×10^{-6} for crystalline copper and 5.9×10^{-6} for α-Zr [15]). It can be seen that: (i) for a given composition, the values of α_m are the same in the amorphous and crystalline states (within the experimental error (about $\pm 0.2 \times 10^{-6}$)) and are very close to the calculated values; (ii) the values of α_m increase as the copper content increases.

These results suggest that the cohesion varies smoothly with composition without any substantial change in the nature of bonding, indicating that the amorphous state for these alloys behaves as a solid solution as formerly proposed [7].

These results also seem to be in agreement with those derived by Fritsch et al. [10] from thermal expansion data on $Pd_{30}Zr_{70}$, $Ti_{50}Be_{40}Zr_{10}$ and $Ni_{24}Zr_{76}$. These workers explained their data, within reasonable assumptions, by the Grüneisen equation and the Debye model for the specific heat. The derivative of the Grüneisen equation with respect to temperature yields

$$\alpha_p = \gamma_G \rho \kappa_T c_v / M_0$$

where γ_G is the Grüneisen parameter, ρ is the density, κ_T is the isothermal compressibility, c_v is the molar specific heat and M_0 is the molar weight. Therefore, the variation in α_p should be governed by the temperature dependence of the specific heat. As shown by Cunat [16], the specific heats

TABLE 4

Mean thermal expansion coefficients between 50 and 300 °C of amorphous and crystalline Cu–Zr alloys: comparison with the calculated coefficients

Alloy	$\alpha_m \times 10^6$		
	Amorphous (relaxed) (± 0.2)	Crystalline (± 0.2)	Calculated
$Cu_{33}Zr_{67}$	9.2	9.2	9.4
$Cu_{40}Zr_{60}$	9.9	9.9	10.2
$Cu_{60}Zr_{40}$	11.8	12.6	12.3

of the amorphous and crystalline alloys are very close in the Cu–Zr system. Thus, this could explain the results obtained.

Influence of the chemical composition on glass transition and crystallization temperatures

Tables 2 and 3 show that the initial glass transition and crystallization temperatures increase with copper content. This result is in agreement with previous determinations carried out by differential thermal analysis [7], with compositions ranging from $Cu_{33}Zr_{67}$ to $Cu_{66}Zr_{34}$.

Application of the activation energy spectrum models to dilatometric data

Several models have been proposed in order to explain the structural relaxation processes [17–21].

Van den Beukel et al. [19] have presented an analysis of dilatometric data in terms of a model [20] based on the concepts of topological and chemical short-range order (TSRO and CSRO respectively) where interatomic distances are described in terms of TSRO. Changes in TSRO are regarded as being irreversible as the temperature is increased. That is, the TSRO always changes in a manner which increases the density of the amorphous specimen. In CSRO, the chemical identities of the atoms are taken into account. The degree of CSRO is temperature dependent and thus CSRO changes are reversible with changes in temperature. As discussed by Gibbs [21], this strict division into two categories seems to lack a fundamental basis. Gibbs [21] discussed how, in general, it is not possible to have a change in CSRO without an accompanying change in TSRO. He developed an activation energy spectrum (AES) model based on the work of Primak [22]. The AES formalism can be used to discuss dilatometric data over a wide time–temperature range and thus it embraces the concepts of TSRO and CSRO. Cunat [23] has shown that relaxation in frozen-in systems is a non-linear phenomenon which can be linearized using an appropriate reduced time, and that a relaxation spectrum can be determined by a universal relation deduced from thermodynamic fluctuation theory. Sinning et al. [24] have also discussed how changes in TSRO and CSRO may cause a change in length. Our results are in good agreement with these concepts.

ACKNOWLEDGEMENTS

The authors are grateful to Dr. J. Bigot (CECM, Vitry) for kindly providing the amorphous ribbons studied in this work.

REFERENCES

1 R.O. Suzuki and P.H. Shingu, J. Non-Cryst. Solids, 61–62 (1984) 1003.
2 A. Inoue, T. Masumoto and H.S. Chen, J. Mater. Sci., 20 (1985) 4057.
3 M. Harmelin, Y. Calvayrac, A. Quivy, J. Bigot, P. Burnier and M. Fayard, J. Non-Cryst. Solids, 61–62 (1984) 931.
4 M. Harmelin, A. Sadoc, A. Naudon, A. Quivy and Y. Calvayrac, J. Non-Cryst. Solids, 74 (1985) 107.
5 M.R.J. Gibbs, J.E. Evetts and J.A. Leake, J. Mater. Sci., 18 (1983) 278.
6 M. Harmelin, E. Etchessahar, J. Debuigne and J. Bigot, Thermochim. Acta, 130 (1988) 177.
7 Y. Calvayrac, J.P. Chevalier, M. Harmelin, A. Quivy and J. Bigot, Philos. Mag. B, 48 (1983) 323.
8 J. Bigot, Y. Calvayrac, M. Harmelin, J.P. Chevalier and A. Quivy, in T. Masumoto and K. Suzuki (Eds.), Proc. 4th Int. Conf. on Rapidly Quenched Metals, Vol. II, The Japan Institute of Metals, Sendai, 1982, p. 1463.
9 E. Etchessahar, D. Ansel and J. Debuigne, Mém. Sci. Rev. Métall., 74 (1977) 469.
10 G. Fritsch, P. Löbl and E. Löscher, in S. Steeb and H. Warlimont (Eds.), Rapidly Quenched Metals, Elsevier Science Publishers B.V., 1985, p. 1027.
11 H.S. Chen, in T. Masumoto and K. Suzuki (Eds.), Proc. 4th Int. Conf. on Rapidly Quenched Metals, Vol. I, The Japan Institute of Metals, Sendai, 1982, p. 495.
12 C. Bergman, I. Avramov, C.Y. Zahra and J.C. Mathieu, J. Non-Cryst. Solids, 70 (1985) 367.
13 Z. Altounian, Tu Guo-hua, J.O. Ström-Olsen and W.B. Muir, Phys. Rev. B, 24 (2) (1981) 505.
14 Z. Altounian, Tu Guo-hua and J.O. Ström-Olsen, J. Appl. Phys., 53 (1982) 4755.
15 P. Lehr, in P. Pascal (Ed.), Nouveau Traité de Chimie Minérale, Tome IX, Masson et Cie, Paris, 1963, p. 326.
16 C. Cunat, Thesis, Nancy I, 4 July 1985.
17 A.I. Taub and F. Spaepen, Acta Metall., 28 (1980) 1781.
18 D. Srolovitz, K. Maeda, V. Vitek and T. Egami, Philos. Mag. A, 44 (1981) 847.
19 A. Van den Beukel, S. Van der Zwaag and A.L. Mulder, Acta Metall., 32 (1984) 1895.
20 A. Van den Beukel and S. Radelaar, Acta Metall., 31 (1983) 419.
21 M.R.J. Gibbs, in S. Steeb and H. Watlimont (Eds.), Proc. 5th Int. Conf. on Rapidly Quench :d Metals, Würzburg, 1984, North-Holland, Amsterdam, Vol. I, 1985, p. 643.
22 W. Primak, Phys. Rev., 100 (1955) 1677.
23 C. Cunat, Z. Phys. Chem. Neue Folge, 157 (1988) 419.
24 H.R. Sinning, L. Leonardsson and R.W. Cahn, Int. J. Rapid Solidification, 1 (1984–1985) 175.